OPEN
Original article

Nuclear Medicine Communications

Comparison of ^{81m}Krypton and ^{99m}Tc-Technegas for ventilation single-photon emission computed tomography in severe chronic obstructive pulmonary disease

Robin de Nijs[a], Nienke D. Sijtsema[a,b], Matthijs F. Kruis[c], Claus Verner Jensen[d], Martin Iversen[e], Michael Perch[e] and Jann Mortensen[a]

Introduction **Ventilation and perfusion single-photon emission computed tomography combined with computed tomography (SPECT/CT) is a powerful tool to assess the state of the lungs in chronic obstructive pulmonary disease (COPD). ^{81m}Krypton is a gaseous ventilation tracer and distributes similarly to air, but is not widely available and relatively expensive. ^{99m}Tc-Technegas is cheaper and has wider availability, but is an aerosol, which may deposit in hot spots as the severity of COPD increases. In this study, ^{81m}Krypton and ^{99m}Tc-Technegas were compared quantitatively in patients with severe COPD.**

Methods **The penetration ratio, the heterogeneity index (with and without band filtering for relevant clinical sizes) and hot spot appearance were assessed in eleven patients with severe COPD that underwent simultaneous dual-isotope ventilation SPECT/CT with both ^{99m}Tc-Technegas and ^{81m}Krypton.**

Results **Significant differences were found in the penetration ratio for the medium energy general purpose (MEGP) collimators, but not for the low energy general purpose (LEGP) collimators. The difference in the overall and the band filtered heterogeneity index was significant in most cases. All patients suffered from ^{99m}Tc-Technegas hot spots in at least one lung. Comparison of MEGP ^{81m}Krypton and LEGP Technegas scans revealed similar results as the comparison for the MEGP collimators.**

Conclusion **Caution should be taken when replacing ^{81m}Krypton with ^{99m}Tc-Technegas as a ventilation tracer in patients with severe COPD as there are significant differences in the distribution of the tracers over the lungs. Furthermore, this patient group is prone to ^{99m}Tc-Technegas hot spots and might need additional scanning if hot spots severely hamper image interpretation.**

Nuclear Medicine Communications 2021, **42**:160–168

Keywords: chronic obstructive pulmonary disease, heterogeneity, Krypton, penetration, single-photon emission computed tomography combined with computed tomography, Technegas, ventilation

[a]Department of Clinical Physiology, Nuclear Medicine and PET, Rigshospitalet, Copenhagen University Hospital, Copenhagen, Denmark, [b]Department of Physics and Astronomy, Faculty of Science, VU University, Amsterdam, The Netherlands, [c]Clinical Science, Philips Healthcare, [d]Department of Radiology, Rigshospitalet, Copenhagen University Hospital and [e]Department of Cardiology, Rigshospitalet, Copenhagen University Hospital, Copenhagen, Denmark

Correspondence to Robin de Nijs, MSc, PDEng, PhD, Copenhagen University Hospital, Blegdamsvej 9, 2100 Copenhagen, Denmark
Tel: +45 35454011; e-mail: robin.de.nijs@regionh.dk

Received 19 May 2020 **Accepted** 23 September 2020

Introduction

Chronic obstructive pulmonary disease (COPD) is a leading cause of morbidity and mortality [1]. It is characterized by inflammation and obstruction of conducting airways, causing an increase in airway resistance. Furthermore, reduced elastic recoil due to destruction of alveolar tissue in combination with exhalation resistance causes hyperinflation of the lungs. Conventionally, the severity of COPD is assessed by spirometry and is reflected in, for example, reduced forced expiratory volume in 1 second, increased total lung capacity and increased residual volume. Due to the fact that COPD affects patches of the lungs and not necessarily a whole lung or lobe, it is a heterogeneous disease. This heterogeneous ventilation pattern is one of the characteristics of COPD seen in ventilation and perfusion (V/Q) single-photon emission computed tomography combined with computed tomography (SPECT/CT). In V/Q SPECT images, COPD appears as matched V/Q defects and/or reversed V/Q mismatches [2]. The latter meaning both V/Q are impaired, but ventilation is affected more. Currently, V/Q SPECT/CT is mainly used to assess options for lung reduction surgery or bronchial valve placement in patients with COPD, and the corresponding post-operative assessment. Although, the technique, especially the ventilation part, also has a potential for early detection of COPD [3] and grading the disease [4,5].

However, the tracer choice for ventilation SPECT is not always straightforward, as multiple options exist. ^{81m}Krypton is a gaseous tracer with a half-life of 13 seconds and

Supplemental Digital Content is available for this article. Direct URL citations appear in the printed text and are provided in the HTML and PDF versions of this article on the journal's website, www.nuclearmedicinecomm.com.

0143-3636 Copyright © 2020 The Author(s). Published by Wolters Kluwer Health, Inc. DOI: 10.1097/MNM.0000000000001314

is therefore cleared from the lungs by decay faster than by expiration. During tidal breathing, the distribution of ^{81m}Krypton will closely follow the ventilation pattern [6]. ^{81m}Krypton enables simultaneous acquisition with ^{99m}Tc based perfusion tracers, because of their different photon energies of 190 and 140 keV. Yet, the half-life of ^{81m}Krypton's mother isotope ^{81}Rubidium, is only 4.6 hours [7], thereby limiting transport options and thus availability in many centers. Moreover, since the source is usable for only a day, it needs to be produced often, causing it to be relatively expensive.

^{99m}Technetium based aerosols may be a solution as this source lasts the better part of a week, making transport more feasible and lowering the costs. However, aerosols consist of labeled particles suspended in air and distribution in the lung is highly dependent on the particle size. Larger particles have the tendency to deposit in the central airways due to the effect of impaction. Yet, as particle size decreases this poses less of a problem. If particles are sufficiently small they will follow the airflow to the alveoli and distribute there by diffusion [8]. In a comparison between ^{99m}Tc labeled diethylenetriaminepentaacetate (^{99m}Tc-DTPA) and ^{99m}Tc-Technegas, of which the latter has smaller particles than the first, it was indeed seen that ^{99m}Tc-DTPA deposited more centrally than Technegas [9]. Central airway deposition is naturally not an issue for gaseous tracers. Other than particle size, the type of airflow influences aerosol deposition [8]. In case of turbulent airflow particle deposition tends to increase, which is seen at bronchial branching and in COPD patients at obstructive sites. In some cases, particle accumulation is extremely high at those sites and the accumulations are seen as hot spots in the ventilation image. The appearance of hot spots usually increases with COPD severity, as obstruction severity and therefore turbulent airflow increases causing the impaction of the aerosol particles [2].

In order to diminish central airway deposition, it is important to use an aerosol with particles as small as possible. Technegas is a good candidate since the particle size ranges from 30 to 60 nm [10]. In clinical practice, slightly larger particles might appear due to aggregation. Technegas has characteristics of both aerosols and gases. General good agreement was shown between the gaseous ^{81m}Krypton and the ultra-fine aerosol Technegas in a number of studies [11–13]. However, these studies were carried out on healthy volunteers, nonobstructive lung disease patients and patients with mild obstructive disease in a mixed group. No previous studies have included patients with severe COPD, although the differences between Technegas and ^{81m}Krypton are expected to be most apparent in this patient group. Therefore, the aim of the current study was to quantitatively compare ^{81m}Krypton and Technegas scans in patients with severe COPD in terms of penetration to the peripheral airways and heterogeneity information contained in the images and to assess the occurrence of hot spots in the Technegas scans.

Methods

Subjects and acquisition

This study is part of a clinical study [14] about valve placement treatment of 11 patients suffering from severe COPD selected on their assessed operability and expected outcome. The Regional Scientific Ethical Committee approved the clinical study (reference no. H-4-2011-047) and written informed consent was obtained from all subjects. All patients, see the summarized characteristics in Table 1, were referred for advanced emphysema treatment with endobronchial valve placement after abstaining smoking for at least 6 months. Before and 6 months after the treatment a V/Q SPECT/CT was performed, where ^{99m}Technetium labeled macroaggregated albumin (MAA) was used as the perfusion tracer and ^{81m}Krypton as the ventilation tracer. The valve procedure is expected to influence ventilation mostly. Therefore, 1 and 3 months after the procedure the ^{81m}Krypton and Technegas ventilation SPECT/CT-scans were performed simultaneously. A lung function test was performed directly prior to the scans, unless it could not be tolerated by the patient. Administered activities (effective dose) were typically 150–300 MBq for ^{81m}Krypton (0.1–0.2 mSv) and 40 MBq [2] for Technegas (0.6 mSv). The SPECT/CT protocol started with a 140 kVp 5 mm slices 20 mAs low-dose CT with dose modulation (1 mSv), 512 × 512 matrix and 1.17 mm isotropic pixel size, after which the dual-isotope ventilation SPECT was acquired (64 × 64 matrix, 64 angles, 12 seconds per angle in step and shoot mode, 9.3 mm isotropic voxels, energy windows at 190.5 and 140.5 keV with 20% width). Prior to the start of the ventilation scan, Technegas was inhaled during three deep breaths, allowing the particles to settle in the lung tissue, before starting the scan. ^{81m}Krypton was inhaled by free tidal breathing during the ventilation scan, allowing for simultaneous imaging of Technegas and ^{81m}Krypton. The first scanning protocol was performed with low energy general purpose (LEGP) collimators. Next, typically after

Table 1 Summary of characteristics from the lung function test of the included patients at the first follow-up

Total number	Age (years)	FEV_1	FVC	FEV_1/FVC (%)	TLC	RV	DLCOc
11 (3F)	60 ± 9	27 ± 11	62 ± 21	35 ± 11	130 ± 13	254 ± 53	33 ± 13

All values are shown as the mean ± the sample SD. Unless stated otherwise % of predicted is stated.
DLCOc, diffusing capacity of lungs for carbon monoxide (corrected for hemoglobin); FEV_1, forced expired volume in the first second; FVC, forced vital volume; RV, residual volume; TLC, total lung capacity.

Table 2 Some relevant available collimator specifications according to the vendor for the Philips Precedence single-photon emission computed tomography combined with computed tomography

Collimator name	Planar resolution, mm at 10 cm	Tc-99m sensitivity (cps/MBq)	Septal thickness (mm)	Septal penetration (%)	Photon energy (keV)
MEGP	11.3	98	1.143	3.3	300
LEGP	8.8	119	0.180	1.9	140
LEHR	7.4	66	0.152	1.3	140

Parameters are defined according to NEMA NU 1-2012.
LEGP, low energy general purpose; LEHR, low energy high resolution; MEGP, medium energy general purpose.

half an hour, the SPECT/CT protocol was repeated with medium energy general purpose (MEGP) collimators. In total, the imaging acquisition itself takes approximately two times 7 minutes. LEGP collimators were preferred over LEHR collimators [2,15] because of the slightly higher septal thickness for minimizing ^{81m}Krypton artifacts and higher sensitivity. Both low and medium energy collimators were investigated, since medium energy is optimal for ^{81m}Krypton, while low energy is optimal for Technegas. The collimator specifications are summarized in Table 2. All scans were performed on a dual-head 16-slice CT Philips Precedence SPECT/16MDCT scanner (Philips Healthcare, Best, the Netherlands) with 9.5-mm-thick-NaI(Tl)-scintillation crystals.

Image reconstruction

Data were reconstructed on a Philips Intellispace 7 workstation, using the Astonish reconstruction algorithm with four iterations and 16 subsets. Three reconstructions were made for each tracer and each set of collimators using different image corrections; no corrections (NAC), attenuation correction only (AC), and both attenuation and scatter correction (ACSC), resulting in six different reconstructions from one scanning session for each tracer. For attenuation correction, the low-dose CT was used [16] and scatter correction was done using the scatter kernel-based effective scatter source estimation (ESSE) as available on the scanner [17]. The ESSE scatter correction does not correct for downscatter from ^{81m}Krypton into the ^{99m}Technetium window.

Image analysis

Volumes of interest (VOIs) were manually drawn by a skilled operator and subsequently controlled by an expert in nuclear medicine lung studies. Both right lung and left lung were drawn separately for all patients and subsequently saved as masks with a value one inside the lung, and zero outside the lung. All VOIs were based on the low-dose CT in combination with the NAC ^{81m}Krypton reconstruction. For both lungs, both sets of collimators and all reconstruction options the penetration ratio, heterogeneity index and scatter plots were computed in MATLAB R2015b (MathWorks Inc., Natick, Massachusetts, USA).

Penetration ratio

The penetration ratio characterizes the ability of the ventilation tracer to reach the lung periphery. As a first step, the relative center denoted by subscript C of the mask $M = M(x, y, z)$ was found by applying the weighted average in each of the three directions of the mask. For the x-direction and analogously for the other directions the center is given by

$$x_C = \frac{\sum x \cdot M}{\sum M}, \tag{1}$$

where M denotes the value of the mask at a certain position, which is either 1 or 0.

Next, the edge voxels of the mask were found by finding all voxels in the mask that had at least one 3D 6-connected neighbor not included in the mask. Subsequently, a radial transform of the lung was carried out, as was proposed by Fleming *et al.* [18]. The fractional radius r_f of each voxel was determined by:

$$r_f = \frac{r}{r_{edge}}, \tag{2}$$

where r_{edge} denotes the radius of the closest edge voxel in terms of the spherical angles θ and φ, and r denotes the radius of the current voxel. Consequently, the origin voxel has a fractional radius of zero and the edge voxels have a fractional radius of one. Voxels with a fractional radius from 0 to 0.5 were included in the central zone and voxels with a fractional radius from 0.8 to 1 were included in the peripheral zone [19]. Figure 1a shows an example of a mask for one axial slice. Figure 1b shows the distribution of fractional radiuses over this axial slice. Next, the penetration ratio (PR) [11] was calculated using:

$$\mathrm{PR} = \frac{c_{peripheral}}{c_{central}} \tag{3}$$

where $c_{peripheral}$ denotes the count average per voxel in the peripheral zone and $c_{central}$ denotes the count average per voxel in the central zone. Figure 1c shows an example of the division of peripheral and central zone in the same axial slice as in Fig. 1a and b.

Heterogeneity index

The heterogeneity of the ventilation was assessed by calculating the coefficient of variance, also called the heterogeneity index [11]. First, it was calculated for

Fig. 1

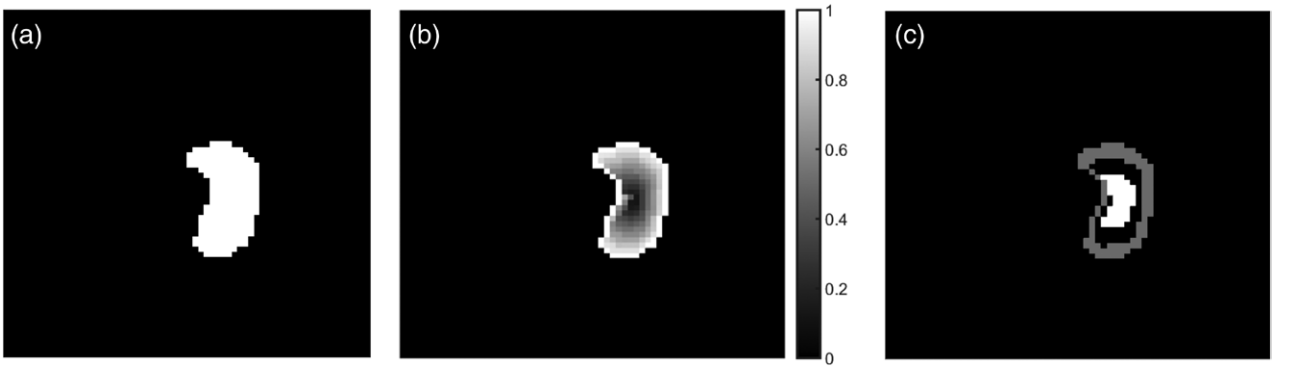

Example of the definition of periphery and center for an axial slice of the left lung for calculation of the penetration ratio. (a) Shows the mask as fits onto the SPECT data. (b) Shows the distribution of fractional radiuses over the mask indicated by the grayscale. The center with a fractional radius of zero is displayed with black inside the lung. (c) Shows the resulting division of the mask in central zone, shown in white, and the peripheral zone, shown in gray.

inhomogeneities of all sizes, in this paper called the overall heterogeneity index, by dividing the SD of counts by the mean of the counts in one VOI.

$$\mathrm{HI} = \frac{\mathrm{SD}}{\mathrm{mean}} \tag{4}$$

Second, it was calculated for inhomogeneities from 2-4 cm, which was arbitrarily chosen to correspond to the apparent size of secondary lobules in ventilation scans while taking into account patient motion [20,21]. In this article, it is referred to as the filtered heterogeneity index, or indicated with index 2–4 cm. For this purpose, the images were filtered before the coefficient of variance was calculated. This also reduces the potential influence of noise on the heterogeneity index.

For this purpose, a Butterworth bandpass filter $B(f)$ was constructed by combining a high-pass and a low-pass to apply to the data. The low-pass filter was defined as [22]:

$$B(f)^{-2} = 1 + \left(\frac{f}{f_c}\right)^{2n} \tag{5}$$

with f_c the cutoff frequency in cm^{-1}, n the order. For taking into account different FOV-sizes in the three directions the frequency f in cm^{-1} was calculated with

$$f^2 = \left(\frac{f_x \cdot N_x}{FOV_x}\right)^2 + \left(\frac{f_y \cdot N_y}{FOV_y}\right)^2 + \left(\frac{f_z \cdot N_z}{FOV_z}\right)^2, \tag{6}$$

where $f_{x,y,z}$ denotes the frequency relative to the sampling frequency d^{-1} with d the pixel size in cm for the three directions. N denotes the number of voxels and FOV denotes the FOV size. The high pass filter was defined as 1 minus the low pass filter. A sixth order ($n = 6$) filter was chosen as a balance between steep and smooth and the cut off frequencies were 0.125 cm^{-1} for the high pass filter and 0.25 cm^{-1} for the low pass filter, corresponding to the first harmonic of the relevant structure sizes of 2–4 cm.

Scatter plots

For each lung in every subject, a scatter plot was generated to compare ^{81m}Krypton and Technegas voxel-by-voxel and to assess hot spot appearance in Technegas scans. Since hot spots are known to have extremely high activity relative to the rest of the lung, statistically significant outliers were detected as an indication of hot spot presence. To this end, a robust linear fit was applied to the data. The root mean square error of Technegas values was calculated to yield a Technegas SD with respect to the fit. The outlier limit was constructed based on a one-tailed Bonferroni corrected z-test (with significance assumed for $P < 0.05$).

Statistical analysis

Even though only 11 patients were selected for this study, the planned number of samples was four times larger, since each individual lung was analyzed and each patient was scanned in two follow-ups. Statistical analysis for comparison of ^{81m}Krypton and Technegas was carried out by performing two-tailed paired Student's *t*-tests, where the pairs consisted of the voxel values(intensities) based on the simultaneously acquired images for the two tracers. Additionally, a paired two-tailed Student's *t*-test was performed for the comparison of ^{81m}Krypton MEGP data with Technegas LEGP data. In this case, the same patients were included as in the comparison for the MEGP collimators. A one-tailed z-test was performed for detection of outliers, assuming an underlying normal

distribution. Significance was assumed at $P < 0.05$ (after Bonferroni correction with the number of voxels for multiple comparisons) in all cases.

Results

Four patients did not have MEGP data at the first follow-up, as these patients were unable to tolerate the second ventilation scan. At the second follow-up, 3 months after the bronchoscopic procedure, one patient opted out of the study. Therefore, seven patients had MEGP data at the first follow-up and 10 patients at the second follow-up. LEGP data were obtained from 11 patients at the first follow-up and 10 patients at the second follow-up. In Tables 3 and 4, the penetration ratio and heterogeneity indices are calculated for pooled data of both lungs and both follow-ups consisting of 34 and 42 samples for MEGP and LEGP, respectively. Tables with the separate results can be found in the supplementary material, supplement digital content 1, *http://links.lww.com/NMC/A179*. Since this study's aim is to compare the two tracers and not patient condition it is considered natural to combine the follow-ups from different time points.

Penetration ratio

Table 3 shows the penetration ratio including the SEM for all reconstructions in patients for both lungs and both follow-ups combined. Note that while all MEGP penetration ratios differ significantly, none of the penetration indices differ significantly for the LEGP collimators. The comparison of ^{81m}Krypton MEGP with Technegas LEGP, included in Table 5, does however yield a significant difference. For all significant differences, the penetration ratio of Technegas is lower than that of ^{81m}Krypton. A Bland–Altman plot comparing the ^{81m}Krypton and Technegas penetration ratio in both collimators is shown in Fig. 2.

Heterogeneity index

Table 4 shows the overall heterogeneity index and filtered heterogeneity index including the SEM for all reconstructions per collimator type in patients for both lungs and both follow-ups combined. Note that the heterogeneity index significantly differs in all cases, except for the overall heterogeneity index in NAC data in the MEGP collimators. The comparison of ^{81m}Krypton MEGP with Technegas LEGP data is included in Table 5 and shows the same pattern as the comparison in the MEGP collimators. Furthermore, significance is higher in all cases for the LEGP collimators than for the MEGP collimators. For all significant differences, the heterogeneity of Technegas is higher than that of ^{81m}Krypton. Bland–Altman plots comparing the ^{81m}Krypton and Technegas heterogeneity index in both collimators are shown in Fig. 3.

Scatter plots

All patients showed outliers in at least one lung in each reconstruction for both of the collimator sets. The maximum amount of outliers for the LEGP NAC and the LEGP AC reconstructions was 88 voxels, while it was

Table 3 Summary of the penetration ratio values for ^{81m}Krypton and Technegas for all reconstructions

	MEGP			LEGP		
Penetration ratio (±SEM)	^{81m}Krypton	Technegas	*P* value	^{81m}Krypton	Technegas	*P* value
ACSC	1.03 ± 0.10	0.84 ± 0.09	3×10^{-4}[a]	0.89 ± 0.03	0.83 ± 0.06	0.18
AC	1.06 ± 0.09	0.88 ± 0.10	7×10^{-4}[a]	0.94 ± 0.03	0.88 ± 0.06	0.16
NAC	0.83 ± 0.06	0.66 ± 0.05	2×10^{-5}[a]	0.73 ± 0.02	0.68 ± 0.04	0.09

AC, attenuation correction; ACSC, attenuation and scatter correction; LEGP, low energy general purpose; MEGP, medium energy general purpose; (N)AC, (non)attenuation corrected; SC, scatter corrected.
[a]Indicate the significant differences between ^{81m}Krypton and Technegas.

Table 4 Summary of the overall heterogeneity index and the filtered heterogeneity index values for ^{81m}Krypton and Technegas for all reconstructions

	MEGP			LEGP		
Heterogeneity Index (±SEM)	^{81m}Krypton	Technegas	*P* value	^{81m}Krypton	Technegas	*P* value
ACSC						
Overall	1.03 ± 0.04	1.18 ± 0.07	0.006[a]	0.71 ± 0.03	1.24 ± 0.07	3×10^{-11}[a]
2–4 cm	0.38 ± 0.02	0.55 ± 0.03	3×10^{-7}[a]	0.19 ± 0.01	0.57 ± 0.04	1×10^{-15}[a]
AC						
Overall	0.98 ± 0.04	1.11 ± 0.06	0.009[a]	0.69 ± 0.03	1.17 ± 0.06	5×10^{-11}[a]
2–4 cm	0.34 ± 0.02	0.51 ± 0.03	2×10^{-7}[a]	0.18 ± 0.01	0.53 ± 0.03	2×10^{-15}[a]
NAC						
Overall	1.02 ± 0.04	1.08 ± 0.06	0.22	0.68 ± 0.02	1.12 ± 0.06	4×10^{-10}[a]
2–4 cm	0.37 ± 0.02	0.50 ± 0.03	1×10^{-5}[a]	0.19 ± 0.01	0.50 ± 0.03	2×10^{-15}[a]

AC, attenuation correction; ACSC, attenuation and scatter correction; LEGP, low energy general purpose; MEGP, medium energy general purpose; (N)AC, (non)attenuation corrected; SC, scatter corrected.
[a]Indicate the significant differences between ^{81m}Krypton and Technegas.

90 for the LEGP ACSC reconstruction. The maximum amount of outliers found in the MEGP data was 89, 87 and 90 voxels for the NAC, AC and ACSC reconstructions, respectively. All maximum amounts of outliers were found in the same patient. Figure 4 shows an example of outliers in a scatter plot corresponding to hot spots in the left lung.

Discussion

Due to the fact that ^{81m}Krypton and Technegas were imaged simultaneously, the difference in medical information in both scans is only due to the difference in the tracers. Therefore, the comparison of these two images does not require any registration and they can be readily compared one-on-one. However, because simultaneous dual-isotope scanning is used, downscatter from ^{81m}Krypton appears in the Technegas window, which is not accounted for in the ESSE scatter correction. Due to this downscatter, Technegas images might be blurred. Yet, the ventilation distribution seen on Technegas images could lead to a bigger observed correlation between ^{81m}Krypton and Technegas, since the downscatter originates from the reference tracer. It might be beneficial to use an energy window scatter correction to be able to account for downscatter, as, for example, for ^{177}Lu [23] or for Krypton and ^{99m}Tc-MAA [24]. Nevertheless, significant differences were found in the majority of the results presented here. Furthermore, by adding attenuation and scatter correction, the values of both penetration ratio and heterogeneity index change, for both tracers with both collimators. This change emphasizes the importance of applying proper corrections for quantitative imaging.

The simultaneous dual-isotope ventilation scans were done for two collimator sets, first LEGP, followed by MEGP. The low energy collimators are the most ideal collimators to image ^{99m}Technetium-based tracers due to the energy range of these collimators. As mentioned before, ^{81m}Krypton energy is higher than ideal for low energy collimators leading to septal penetration, which severely degrades the image quality by causing blurring. As can be seen from Tables 3 and 4 Technegas values for the penetration ratio(PR) and heterogeneity index (HI) are very close for both collimators. This is not the case for ^{81m}Krypton, where there are large differences in the values depending on the collimator. To yield a better quality ^{81m}Krypton image, the medium energy collimators

Table 5 Summary of the paired analysis for HI and PR comparing ^{81m}Krypton with medium energy general purpose collimators and Technegas with low energy general purpose collimators

	^{81m}Krypton	Technegas	
(±SEM)	MEGP	LEGP	*P* value
ACSC			
HI Overall	1.03 ± 0.04	1.20 ± 0.07	0.004[a]
HI 2–4 cm	0.38 ± 0.02	0.56 ± 0.04	1×10^{-6}[a]
PR	1.03 ± 0.1	0.78 ± 0.06	3×10^{-5}[a]
AC			
HI Overall	0.98 ± 0.04	1.13 ± 0.07	0.007[a]
HI 2–4 cm	0.34 ± 0.02	0.51 ± 0.04	9×10^{-7}[a]
PR	1.06 ± 0.1	0.83 ± 0.07	3×10^{-5}[a]
NAC			
HI Overall	1.02 ± 0.04	1.08 ± 0.06	0.26
HI 2–4 cm	0.37 ± 0.02	0.49 ± 0.03	4×10^{-5}[a]
PR	0.83 ± 0.06	0.64 ± 0.04	5×10^{-6}[a]

[a]Indicate the significant differences between ^{81m}Krypton and Technegas.
AC, attenuation correction; ACSC, attenuation and scatter correction; HI, heterogeneity index; (N)AC, (non)attenuation corrected; PR, penetration ratio; SC, scatter corrected; LEGP, low energy general purpose; MEGP, medium energy general purpose.

Fig. 2

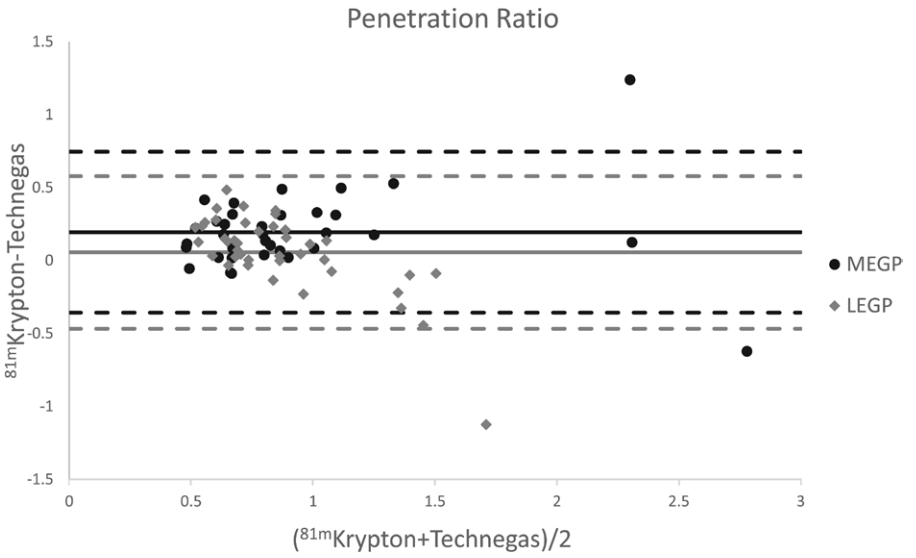

Bland–Altman plot of the PR for ^{81m}Krypton versus Technegas, for MEGP and LEGP collimators. Attenuation and scatter correction were applied. The dashed lines indicate 1.96 SD. LEGP, low energy general purpose; MEGP, medium energy general purpose; PR, penetration ratio.

are normally used to limit septal penetration, however, these collimators have a lower resolution. Therefore, one of the two simultaneous ventilation images is always sub-optimal. However, the severity of the septal penetration usually outweighs the severity in decrease of sensitivity and resolution.

Fig. 3

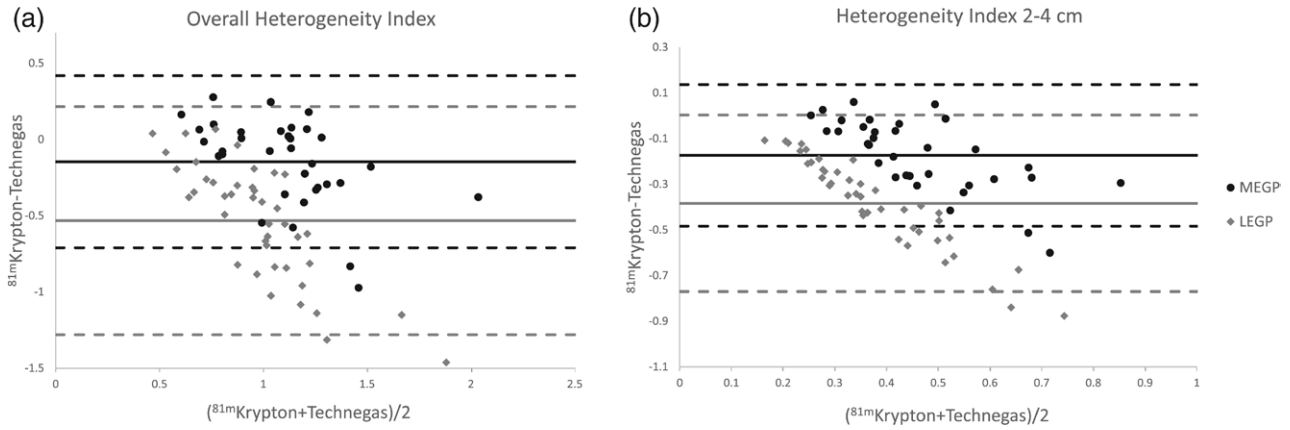

Bland–Altman plots of ^{81m}Krypton versus Technegas for the overall HI (a) and filtered HI (b) after application of ACSC. ACSC, attenuation and scatter correction; HI, heterogeneity index.

Fig. 4

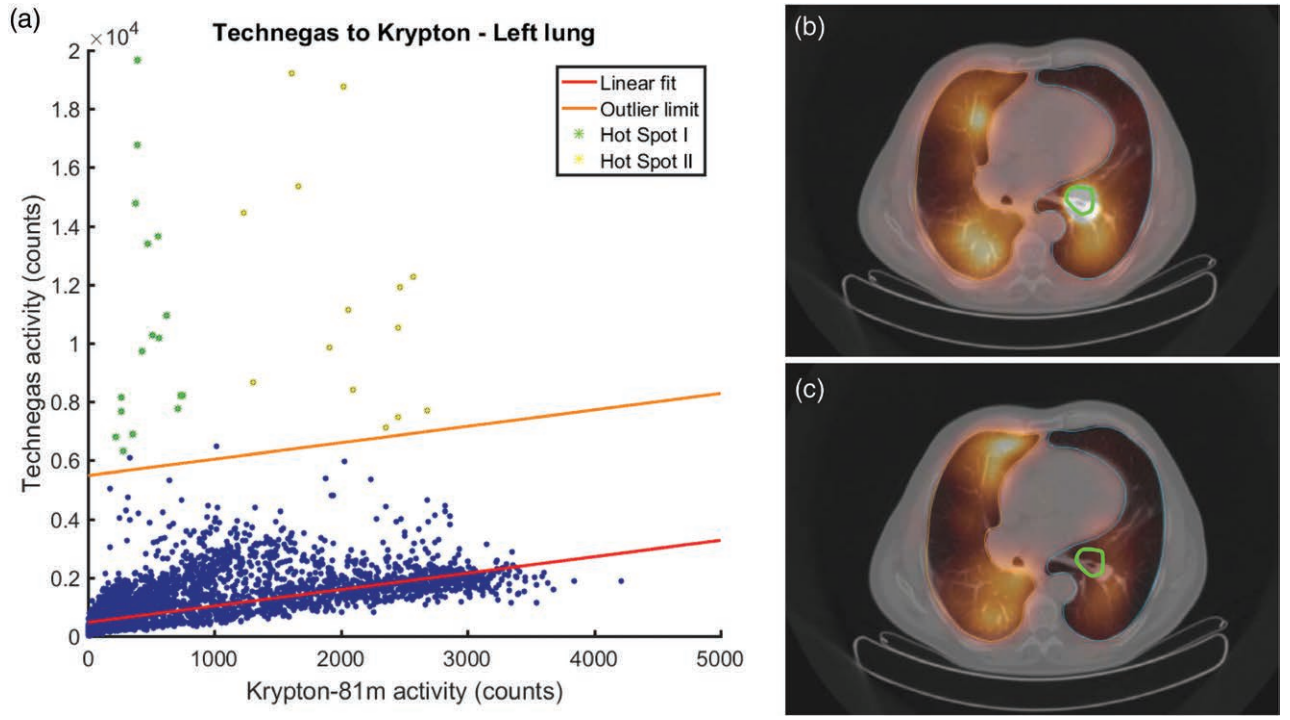

An example of a patient with a severe hot spot in the left lung for Technegas in an attenuation and scatter corrected scan using MEGP collimators. (a) The scatter plot corresponding to the left lung showing 33 outliers. The red line indicates the linear fit, while the orange line indicates the outlier limit; all points above the outlier limit are considered to be statistically significant outliers. (b) An axial slice of the corresponding Technegas ventilation image and (c) the same slice in the corresponding ^{81m}Krypton ventilation image. Note the presence of a severe hot spot in the center of the left lung in the Technegas scan outlined in the ROI marked in green (b). The ROI is an autocontour based on 40% of the maximum Technegas intensity. Points in this hot spot ROI are indicated in green in the scatterplot (a). The other hot spot, indicated in the scatter plot in yellow, is not shown in the axial slices. In (b) and (c), the right lung is outlined in orange and the left lung is outlined in blue. MEGP, medium energy general purpose.

Significant differences between ^{81m}Krypton and Technegas were found for the penetration ratio in the MEGP collimators in all reconstructions, in which case the PR was higher for ^{81m}Krypton in all cases. The same was observed when comparing ^{81m}Krypton with MEGP collimators with Technegas with LEGP collimators. This is in line with expectations, since aerosols have the tendency to deposit more in the central airways and at airflow obstruction sites than in the peripheral airways. Additionally, hot spots in Technegas scans are more likely to appear in the central airways, resulting in a lower PR for Technegas. There were no significant differences in the PR when comparing ^{81m}Krypton and Technegas in the LEGP collimators. This is probably due to the septal penetration in the ^{81m}Krypton images.

It is expected that the penetration ratio is around one to signify a relatively even distribution over central and peripheral lung tissue. However, in this study, one patient showed very high (>2) PR for both ^{81m}Krypton and Technegas in AC(SC) MEGP data and for Technegas in LEGP AC(SC) data, meaning the tracer deposited more in the periphery than in the central part of the lung. This pattern coincided with the pattern of the severe emphysema, which was mainly present in the central area of one lung, while the periphery was in better shape.

The heterogeneity index showed significant differences between ^{81m}Krypton and Technegas in most cases for both collimators. Additionally, when comparing ^{81m}Krypton in MEGP collimators and Technegas in LEGP collimators the same pattern was observed. In all cases, the mean HI is larger for the overall heterogeneity index than for the filtered HI. This is to be expected since the filtering removes slow spatial variations as well as fast spatial variations, effectively decreasing the overall amount of variations present in the scan. Furthermore, it is notable that the significance increases when looking at clinically relevant sizes of heterogeneities (2–4 cm, similar to the size of the secondary lobules of the lungs plus a motion margin), indicating the difference between the two ventilation tracers is even more relevant for the spatial variations that are clinically interesting. The HI for Technegas is very similar for both collimators, but not for ^{81m}Krypton. As for PR, this is probably due to the septal penetration in the ^{81m}Krypton images, which results in blurring and therefore a lower HI is observed.

Values for the overall HI are close to one, which would mean that the SD is close to the value of the mean for normal distributions. However, additional to the heterogeneous ventilation seen in COPD patients, Technegas scans include hot spots. Since hot spots have a value far above the mean, their appearance will lead to a high SD and therefore higher HI. The HI and SD for the areas without hot spots will be lower, as is the case for healthy subjects without hot spots. Heterogeneous ventilation is one of the characteristics of COPD [25].

Previously, two studies have also reported the potential of heterogeneity measure in V/Q SPECT/CT as a tool for COPD grade assessment with Technegas. Bajc *et al.* [5] reported it was possible to grade COPD patients and healthy long-time smokers by V/Q SPECT/CT by using a qualitative approach [5]. A quantitative method for heterogeneity assessment was also reported by Norberg *et al.* [4] who were able to distinguish between healthy subjects and COPD patients. However, Technegas scans are expected to show a higher degree of heterogeneity due to appearance of hot spots in severe COPD and the method presented by Norberg *et al.* [4] was more complicated than the one used here. Therefore, more research is necessary to determine whether the HI used in this study is sufficiently powerful, especially for ^{81m}Krypton, to distinguish between different grades of COPD. Additionally, reference values for the HI of varying grades of COPD should be obtained for the different ventilation tracers, since significant differences were found between ^{81m}Krypton and Technegas.

In this study all patients showed mild to severe Technegas hot spots, indicating a higher risk of hot spot deposition in this patient group than in the mixed patient groups reported previously, where hot spots occurred in 36 [26] and 50% [27] of the patients, respectively. However, James *et al.* [27] did note hot spots were mainly found in patients with obstructive lung disease. When hot spots are present, the quality of the Technegas image is negatively influenced, as less activity is left to spread to ventilated areas outside the hot spot. Also, the corresponding non-ideal scaling makes it difficult to interpret images correctly.

In the current study, hot spot detection was done by finding outliers based on a linear fit. Although the majority of the data showed an acceptable linear pattern, a linear fit might not be the best choice for all of the data. In the case that a percentage of tracer is deposited every unit of distance, for example, a parabolic fit through the origin might be a better option. Additionally, not all outliers necessarily belong to a hot-spot as can be seen in Fig. 2. To improve the accuracy of the hot spot detection a more precise definition of a hot spot or hot spot severity needs to be determined. This could for example include constraints on the average distance between outliers and the outlier limit, or the spread between outliers. However, it should be noted that in clinical practice only one ventilation tracer is used for ventilation imaging. In the case of Technegas, there is no reference scan without hot spots available that could fulfill the role of ^{81m}Krypton in the used scatter plots. Therefore, it would be beneficial to investigate strategies for the (automatic) detection and correction or removal of hot spots in Technegas SPECT/CT images, to avoid the need for additional imaging.

Conclusion

Comparison of ^{81m}Krypton and Technegas (and also V/Q SPECT with ^{81m}Krypton and ^{99m}Tc-MAA) in

simultaneous dual-isotope ventilation SPECT is best performed with medium energy collimators. Penetration ratio and Heterogeneity Index for ^{81m}Krypton and Technegas were significantly different in most cases. Also, hot spots may appear in the Technegas images. Therefore, caution should be taken when replacing ^{81m}Krypton with Technegas, especially in patients with severe COPD. However, Technegas hot spots might have some diagnostic value showing obstructive sites in COPD. In studies monitoring the progress of ventilation, the same radiotracer should be used. ^{81m}Krypton seems to be the better ventilation radiotracer, because of the better penetration and lack of hot spots.

Acknowledgements

N.D.S. received an Erasmus+ grant for 100 days from the European Commission.

The Regional Scientific Ethical Committee approved the study (reference no. H-4-2011-047). Written informed consent was obtained from all subjects.

Conflicts of interest

There are no conflicts of interest.

References

1 Mannino DM, Braman S. The epidemiology and economics of chronic obstructive pulmonary disease. *Proc Am Thorac Soc* 2007; **4**:502–506.
2 Bajc M, Neilly JB, Miniati M, Schuemichen C, Meignan M, Jonson B. EANM guidelines for ventilation/perfusion scintigraphy: part 1. Pulmonary imaging with ventilation/perfusion single photon emission tomography. *Eur J Nucl Med Mol Imaging* 2009; **36**:1356–1370.
3 Norberg P, Persson HL, Schmekel B, Carlsson GA, Wahlin K, Sandborg M, Gustafsson A. Does quantitative lung SPECT detect lung abnormalities earlier than lung function tests? Results of a pilot study. *EJNMMI Res* 2014; **4**:39.
4 Norberg P, Persson HL, Carlsson GA, Bake B, Kentson M, Sandborg M, Gustafsson A. Quantitative lung SPECT applied on simulated early COPD and humans with advanced COPD. *EJNMMI Res* 2013; **3**:28.
5 Bajc M, Markstad H, Jarenbäck L, Tufvesson E, Bjermer L, Jögi J. Grading obstructive lung disease using tomographic pulmonary scintigraphy in patients with chronic obstructive pulmonary disease (COPD) and long-term smokers. *Ann Nucl Med* 2015; **29**:91–99.
6 Valind SO, Rhodes CG, Jonson B. Quantification of regional ventilation in humans using a short-lived radiotracer–theoretical evaluation of the steady-state model. *J Nucl Med* 1987; **28**:1144–1154.
7 Fazio F, Jones T. Assessment of regional ventilation by continuous inhalation of radioactive krypton-81m. *Br Med J* 1975; **3**:673–676.
8 Bajc M, Neilly B, Miniati M, Mortensen J, Jonson B. Methodology for ventilation/perfusion SPECT. *Semin Nucl Med* 2010; **40**:415–425.
9 Jögi J, Jonson B, Ekberg M, Bajc M. Ventilation-perfusion SPECT with 99mTc-DTPA versus Technegas: a head-to-head study in obstructive and nonobstructive disease. *J Nucl Med* 2010; **51**:735–741.
10 Senden TJ, Moock KH, Gerald JF, Burch WM, Browitt RJ, Ling CD, Heath GA. The physical and chemical nature of Technegas. *J Nucl Med* 1997; **38**:1327–1333.
11 Peltier P, De Faucal P, Chetanneau A, Chatal JF. Comparison of technetium-99m aerosol and krypton-81m in ventilation studies for the diagnosis of pulmonary embolism. *Nucl Med Commun* 1990; **11**:631–638.
12 Cook G, Clarke SE. An evaluation of Technegas as a ventilation agent compared with krypton-81 m in the scintigraphic diagnosis of pulmonary embolism. *Eur J Nucl Med* 1992; **19**:770–774.
13 Hartmann IJ, Hagen PJ, Stokkel MP, Hoekstra OS, Prins MH. Technegas versus (81m)Kr ventilation-perfusion scintigraphy: a comparative study in patients with suspected acute pulmonary embolism. *J Nucl Med* 2001; **42**:393–400.
14 Kristiansen JF, Perch M, Iversen M, Krakauer M, Mortensen J. Lobar quantification by ventilation/perfusion SPECT/CT in patients with severe emphysema undergoing lung volume reduction with endobronchial valves. *Respiration* 2019; **98**:230–238.
15 Bajc M, Schümichen C, Grüning T, Lindqvist A, Le Roux PY, Alatri A, *et al*. EANM guideline for ventilation/perfusion single-photon emission computed tomography (SPECT) for diagnosis of pulmonary embolism and beyond. *Eur J Nucl Med Mol Imaging* 2019; **46**:2429–2451.
16 Khalil MM. Positron emission tomography: basic principles. In: Khalil MM, editor. *Basic Sciences of Nuclear Medicine*. Berlin, Heidelberg: Springer; 2011, pp 201–206.
17 Kadrmas DJ, Frey EC, Karimi SS, Tsui BM. Fast implementations of reconstruction-based scatter compensation in fully 3D SPECT image reconstruction. *Phys Med Biol* 1998; **43**:857–873.
18 Fleming JS, Halson P, Conway J, Moore E, Nassim MA, Hashish AH, *et al*. Three-dimensional description of pulmonary deposition of inhaled aerosol using data from multimodality imaging. *J Nucl Med* 1996; **37**:873–877.
19 Tossici-Bolt L, Fleming JS, Conway JH, Martonen TB. Analytical technique to recover the third dimension in planar imaging of inhaled aerosols: (1) impact on spatial quantification. *J Aerosol Med* 2006; **19**:565–579.
20 Osborne DR, Effmann EL, Hedlund LW. Postnatal growth and size of the pulmonary acinus and secondary lobule in man. *AJR Am J Roentgenol* 1983; **140**:449–454.
21 Seppenwoolde Y, Shirato H, Kitamura K, Shimizu S, van Herk M, Lebesque JV, Miyasaka K. Precise and real-time measurement of 3D tumor motion in lung due to breathing and heartbeat, measured during radiotherapy. *Int J Radiat Oncol Biol Phys* 2002; **53**:822–834.
22 Cooke CD, Faber TL, Galt JR. Fundamentals of image processing in nuclear medicine. In: Khalil MM, editor. *Basic sciences of nuclear medicine*. Berlin, Heidelberg: Springer; 2010, pp 217–257.
23 de Nijs R, Lagerburg V, Klausen TL, Holm S. Improving quantitative dosimetry in (177)Lu-DOTATATE SPECT by energy window-based scatter corrections. *Nucl Med Commun* 2014; **35**:522–533.
24 Bacher T, Klavsen MF. [P084] Tests of down-scatter correction in simultaneously acquired TC-99M perfusion and KR-81M ventilation scans. *Phys Medica* 2018; **52**:S125.
25 Mortensen J, Berg RMG. Lung scintigraphy in COPD. *Semin Nucl Med* 2019; **49**:16–21.
26 Inoue T, Watanabe N, Oriuchi N, Tateno M, Tomiyoshi K, Mitomo O, *et al*. [Clinical evaluation of lung scintigraphy with 99mTc-technegas]. *Nihon Igaku Hoshasen Gakkai Zasshi* 1990; **50**:1590–1600.
27 James JM, Lloyd JJ, Leahy BC, Church S, Hardy CC, Shields RA, *et al*. 99Tcm-Technegas and krypton-81m ventilation scintigraphy: a comparison in known respiratory disease. *Br J Radiol* 1992; **65**:1075–1082.